How Does the Exchange of One Oxygen Atom with Sulfur Affect the Catalytic Cycle of Carbonic Anhydrase?[±]

Stephan Schenk,[a] Jürgen Kesselmeier,[b] and Ernst Anders*[a]

Dedicated to Professor Dr. Eckhard Dinjus on the occasion of his 60th birthday

Abstract: We have extended our investigations of the carbonic anhydrase (CA) cycle with the model system $[(H_3N)_3ZnOH]^+$ and CO_2 by studying further heterocumulenes and catalysts. We investigated the hydration of COS, an atmospheric trace gas. This reaction plays an important role in the global COS cycle since biological consumption, that is, uptake by higher plants, algae, lichens, and soil, represents the dominant terrestrial sink for this gas. In this context, CA has been identified by a member of our group as the key enzyme for the consumption of COS by conversion into CO_2 and H_2S. We investigated the hydration mechanism of COS by using density functional theory to elucidate the details of the catalytic cycle. Calculations were first performed for the uncatalyzed gas phase reaction. The rate-determinig step for direct reaction of COS with H_2O has an energy barrier of $\Delta G = 53.2\ kcal\,mol^{-1}$. We then employed the CA model system $[(H_3N)_3ZnOH]^+$ (**1**) and studied the effect on the catalytic hydration mechanism of replacing an oxygen atom with sulfur. When COS enters the carbonic anhydrase cycle, the sulfur atom is incorporated into the catalyst to yield $[(H_3N)_3ZnSH]^+$ (**27**) and CO_2. The activation energy of the nucleophilic attack on COS, which is the rate-determining step, is somewhat higher ($20.1\ kcal\,mol^{-1}$ in the gas phase) than that previously reported for CO_2. The sulfur-containing model **27** is also capable of catalyzing the reaction of CO_2 to produce thiocarbonic acid. A larger barrier has to be overcome for the reaction of **27** with CO_2 compared to that for the reaction of **1** with CO_2. At a well-defined stage of this cycle, a different reaction path can emerge: a water molecule helps to regenerate the original catalyst **1** from **27**, a process accompanied by the formation of thiocarbonic acid. We finally demonstrate that nature selected a surprisingly elegant and efficient group of reactants, the $[L_3ZnOH]^+/CO_2/H_2O$ system, that helps to overcome any deactivation of the ubiquitous enzyme CA in nature.

Keywords: carbon dioxide fixation · carbonic anhydrase · carbonyl sulfide fixation · density functional calculations · enzyme models

Introduction

Carbonic anhydrase (CA) is a ubiquitous zinc enzyme that accelerates the reversible hydration of CO_2 by a factor of 10^7 as compared to the uncatalyzed reaction.[1] This enzymatic process is very important for all living organisms for the exchange of CO_2 with the atmosphere. In addition to its vital importance in the CO_2 exchange process, CA plays a very significant role in the global regulation of carbonyl sulfide (COS) in the atmosphere since it is the key enzyme for the uptake and consumption of this important atmospheric constituent.[2,3] In this context, COS can clearly be regarded as an important natural substrate for this enzyme.

Of the seven CA isoenzymes found so far,[1g] human carbonic anhydrase II is the most efficient, with a turnover of $10^6\ s^{-1}$ at pH 9 and 25 °C.[1g] The equilibrium position of this very fast (almost diffusion-controlled)[1h] enzymatic reaction is pH dependent. Hydration of CO_2 takes place at pH

[a] Dipl.-Chem. S. Schenk, Prof. Dr. E. Anders
Institute of Organic Chemistry
and Macromolecular Chemistry
Friedrich Schiller University Jena
Humboldtstrasse 10, 07743 Jena (Germany)
Fax: (+49) 3641-948212
E-mail: ernst.anders@uni-jena.de

[b] Prof. Dr. J. Kesselmeier
Max Planck Institute for Chemistry
Biogeochemistry Department, University Campus
P.O. Box 3060, 55128 Mainz (Germany)

[±] Since submission of this article, a very interesting paper (A. Bottoni, C. Z. Lanza, G. P. Miscione, D. Spinelli, *J. Am. Chem. Soc.* **2004**, *126*, 1542) on parts of the carbonic anhydrase cycle has appeared that supports our findings for CO_2. The authors also investigated pocket effects with a larger model system than ours and we are happy to discover that the catalytic mechanism previously calculated by us is basically conserved in this larger model.

 DOI: 10.1002/chem.200305754

values above 7, whereas dehydration of bicarbonate predominates at a pH value of less than 7. The activation barrier for this enzymatic reaction is around 3 kcal mol^{-1}, as deduced from the experimental rate constant.[4] The overall experimental free energy change in the reaction is also minimal, as can be inferred either from the difference between the activation barriers for the forward and reverse reactions (+3.1 kcal mol^{-1})[1h] or from the equilibrium constant (+4.1 kcal mol^{-1}).[5]

The active center of the enzyme contains a single Zn^{2+} cation bound to three imidazole ligands originating from histidine residues (His94, His96, and His119).[6] An additional histidine residue (His64) is ideally positioned in the vicinity of the active site and probably functions as a proton relay for hydrogen migration from a loosely bound carbonic acid molecule to the external medium.[7]

Ever since the earliest proposal of a mechanism for CA in 1971,[8] a continuous stream of research designed to unravel the details of the elusive and intricate mechanism of catalytic CO_2 hydration has been reported in the chemical literature. As well as the numerous experimental studies[1,6,9,20] that have been reported over the years, computer simulations have been carried out that have contributed significantly to our present knowledge of the reaction mechanism. The entire spectrum of computational chemistry, from molecular dynamics[10] to the application of semiempirical methods,[11] as well as ab initio[12] and density functional theory (DFT) calculations[13] has been applied in these investigations. Further important contributions to a detailed understanding of the catalytic activity of this enzyme have been made by experimental investigations of suitable model systems (biomimetic complexes).[14–17]

We recently published a cumulative catalytic cycle[18] for carbonic anhydrase (Scheme 1 and Scheme 2) that profits from more than forty years of research. The cycle is based on the simple biomimetic complex $[(H_3N)_3ZnOH]^+$ (**1**), which is the most thoroughly investigated CA model system

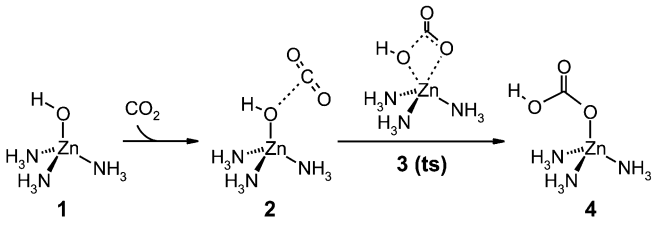

Scheme 1. Catalytic reaction cycle for $[(H_3N)_3\ ZnOH]^+$ (**1**), used as a model of carbonic anhydrase. Part 1: formation of the Lindskog product **4** (adapted from Scheme 2 in reference [18]). ts = transition state.

to date. Our previous B3LYP/6–311 + G(d,p) calculations included entropic and solvent corrections (isodensity surface polarized continuum model[19] with a dielectric constant (ε = 37) between those for the gas phase and water). These calculations revealed that, as CO_2 approaches the catalytic center, an initial encounter complex **2** is formed in which a lone pair of electrons on the zinc-bound hydroxide group interacts with the carbon atom of CO_2. A bicoordinate transition structure **3** leads to the formation of an initial bicarbonate complex **4** (Lindskog intermediate) in which the original Zn–OH bond has been broken (see Scheme 2). There is experimental evidence for the formation of this intermediate by a cobalt-substituted CA mutant.[20] This rate-limiting step in the catalytic cycle has a calculated activation energy in solution of +5.7 kcal mol^{-1};[18] the literature value is around +3 kcal mol^{-1}.[4] The Lindskog intermediate **4** then rearranges through rotation about the C–O(Zn) bond (transition structure **5**) to yield the more stable Lipscomb intermediate **6** (see Scheme 2). A water molecule from the surrounding medium approaches the zinc ion and the hydrated complex **9a** results. No barrier for this process could be found at the B3LYP level of theory. Hydrogen transfer from the water molecule to the carbonyl group considerably weakens the Zn–O(carbonate) bond in the transition state

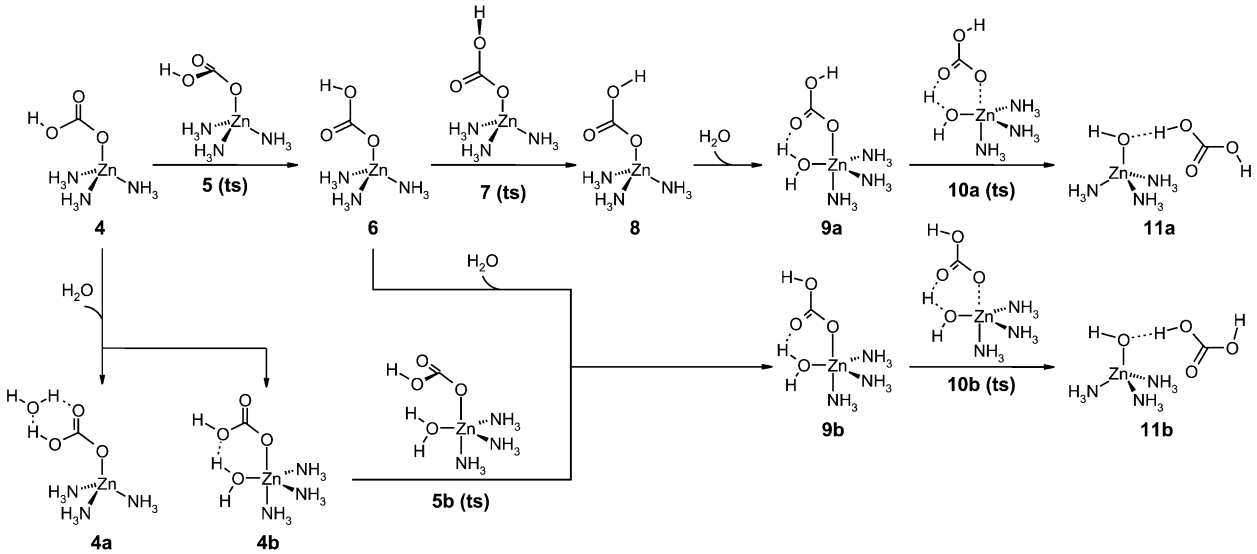

Scheme 2. Catalytic reaction cycle for $[(H_3N)_3\ ZnOH]^+$ (**1**), used as a model of carbonic anhydrase. Part 2: possible reactions of the Lindskog product **4** leading to formation of carbonic acid.

10a and the loosely coordinated carbonic acid/zinc complex **11a** is formed. Deprotonation of the carbonic acid most likely occurs by a proton relay mechanism. The loosely bound bicarbonate can then either dissociate from the active site or undergo an ion-return process before dissociating. Reinvestigation of this catalytic reaction revealed some new aspects of the process that are discussed below.

Variation of the biomimetic complex used to mimic the active site of CA and re-evaluation of the catalytic cycle (albeit at a slightly lower level of theory) demonstrated that the proposed mechanism is valid for a wide range of biomimetic systems.[21] A quantitative structure–activity relationship could even be derived from these computational results, which allows us to estimate the relative reactivity of any given biomimetic $[L_nZnOH]^+$ complex (L, ligand; n, number of ligands) with CO_2 if the Zn–OH bond length is known.[21]

To gain a better understanding of the natural system and to develop novel synthetic methods, we began to study the sulfur analogues of CO_2 (CS_2 and COS). Some initial results for CS_2 have already been published. We recently predicted that a four-center intermediate is involved in the reaction of CS_2 with the biomimetic complex $[(H_3N)_3ZnOH]^+$ (**1**) and this hypothesis has been experimentally verified.[22b,23] Model calculation of CS_2 fixation by **1** results in a much more complicated potential energy surface than that calculated for CO_2 and **1** (more intermediates and reaction paths are involved for CS_2).[23]

We have now extended our studies to consider the unsymmetrical COS molecule. Carbonyl sulfide is the predominant sulfur-containing gas in the troposphere, with a lifetime of between 1–7 years and a remarkably constant atmospheric concentration over the past few decades.[24] This gas contributes to the aerosol particles within the stratospheric aerosol layer[25] as well as to heterogeneous atmospheric chemistry and ozone destruction.[26] Sinks and sources of COS have been under investigation for decades but knowledge in this field is still insufficient, as is strikingly visible in the inconsistent estimates published for these sinks and sources.[2] The dominant sinks, that is, soil and vegetation, involve biologically mediated consumption based on the metabolic hydration of COS by the enzyme carbonic anhydrase. It is of great interest that the carbonic anhydrase species has evolved over time into a prime candidate for taking up and consuming COS from the atmosphere. Investigations involving enzyme isolation, inhibition, and induction experiments with different kinds of organisms have provided evidence that CA, besides its role in CO_2 exchange, is the key enzyme for the uptake and consumption of atmospheric COS and catalyzes the splitting of COS into CO_2 and H_2S.[3]

Parallel to ongoing experimental work in our laboratory, we have also studied the effect on the catalytic cycle when the source of sulfur is the catalyst instead of the cumulene (CO_2 fixation on $[(H_3N)_3ZnSH]^+$).

Results and Discussion

Reaction of CO_2 with $[(H_3N)_3ZnOH]^+$: In a previous paper,[18] we focused on the most stable isomer of carbonic acid. We therefore pursued the path leading to product complex **11a** (Scheme 2). We unintentionally omitted the "true" Lipscomb product **6** and ts **7**, which is formed during reorientation of the hydrogen atom in the bicarbonate moiety to form **8**, the complex previously taken as the Lipscomb product. Herein, we report these missing structures. We have also reinvestigated the steps involved in addition of a water molecule to the central zinc atom. The full pathway and the structures involved are shown in Scheme 2 and Figure 1. Table 1 shows energy values for the pathway. We used the B3LYP/6–311+G(d,p) level of theory for calculations, as in our previous work.[18]

Table 1. Relative Gibbs' free energies and activation barriers for the gas-phase reaction of **1** and CO_2. Calculated at the B3LYP/6–311+G(d,p) level of theory.[a]

	ΔG [kcal mol^{-1}]	ΔG_a [kcal mol^{-1}][b]
1 + CO_2	0.0	–
2	2.6	–
3 (ts)	15.0	15.0
4	9.3	–
4a	7.4	–
4b	10.7	–
5 (ts)	12.2	2.9
5b (ts)	13.1	2.4
6	3.1	–
7 (ts)	13.5	10.4
8	1.7	–
9a	3.8	–
9b	2.4	–
10a (ts)	3.5	–[c]
10b (ts)	2.6	0.2
11a	3.4	–
11b	3.4	–

[a] Some of the data in the table are taken from reference [18]. [b] ΔG_a, activation energy. [c] Due to the intrinsic error of the applied method no significant barrier could be found.

The Lindskog product **4** is the direct result of nucleophilic attack by the zinc-bound hydroxy group on CO_2. It is generally assumed that **4** stabilizes itself either through a rotation about the C–O bond (ts **5**) or by a proton transfer (not shown) yielding the more stable Lipscomb product **6**. Our calculations suggest that an alternative mechanism may exist. Incorporation of an external water molecule is not necessarily restricted to **6**, but could instead occur at an earlier stage of the reaction path.

Addition of a water molecule to the central zinc atom of **4** yields **4b**, which is only slightly destabilized (+1.4 kcal mol^{-1}) compared to **4**. No energy barrier could be found for this process. Alternatively, the water molecule could add to the bicarbonate moiety to form **4a**, which is 1.9 kcal mol^{-1} more stable than **4**. Such a structure would greatly facilitate proton transfer (Lipscomb mechanism) from one oxygen atom to the other since formation of a very unfavorable four-membered ring can be avoided.

Like **4**, structure **4b** can stabilize itself by rotation about the C–O bond to yield **9b** without the involvement of a

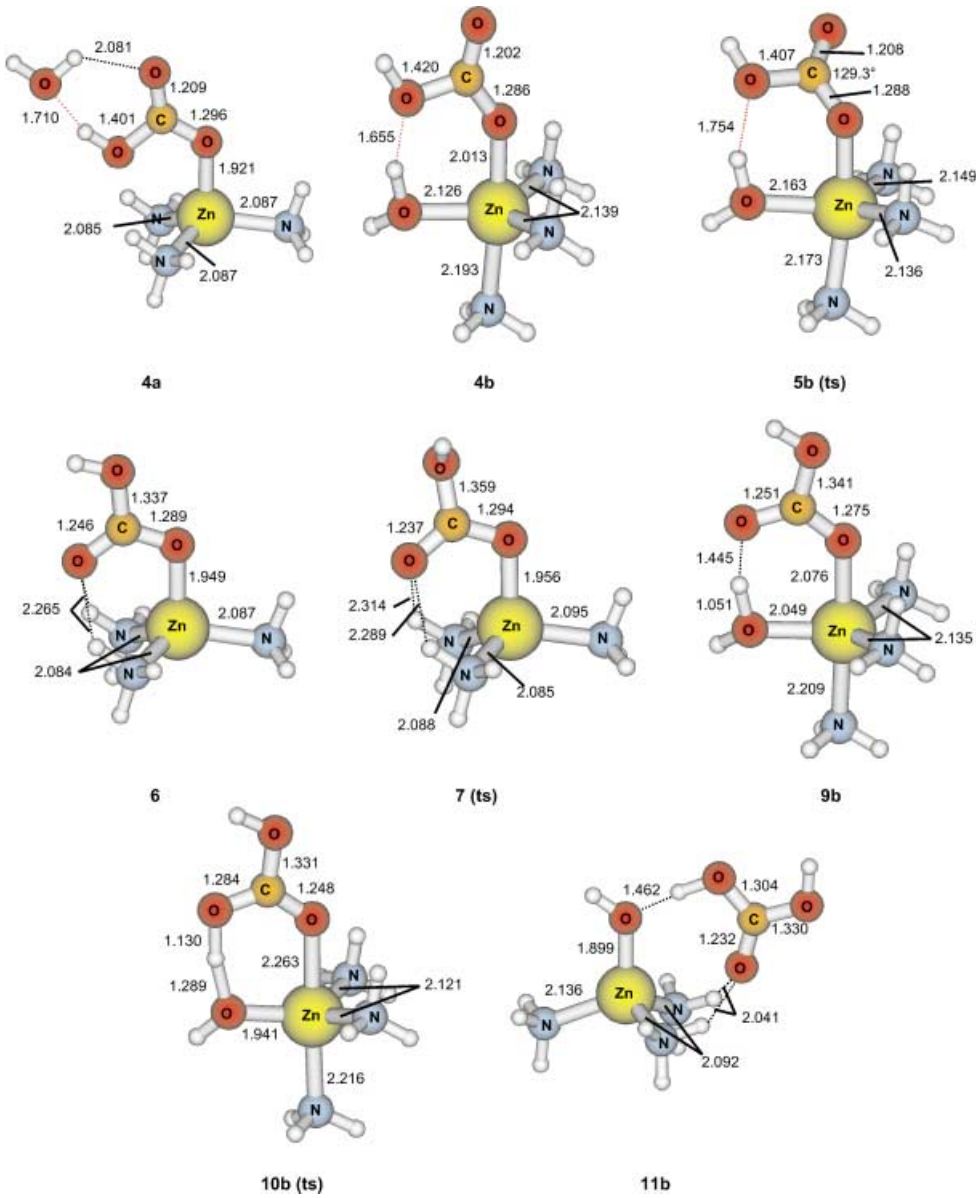

Figure 1. Structures of $[(H_3N)_3ZnOH]^+$ (**1**) at selected stationary points along the reaction coordinate of the reaction with CO_2 (Scheme 2). Bond lengths are given in Å. The structures were calculated at the B3LYP/6–311+G(d,p) level of theory.

Lipscomb-like structure (**6**). The corresponding ts, **5b** (+13.1 kcal mol^{-1}), is very similar in energy to **5** (+12.2 kcal mol^{-1}). The error range of the applied B3LYP method means that we cannot reliably decide which mechanism is the preferred one.

As can be seen from Table 1, formation of **9b** is preferred over formation of **9a**. Structure **9b** can be formed directly from **6** by a barrierless addition of a water molecule, while formation of **9a** from the same complex requires a rather energy-consuming ($\Delta G_a = 10.4$ kcal mol^{-1}) reorientation of the hydrogen atom in the bicarbonate moiety through **7** (+13.5 kcal mol^{-1}). As reported previously,[18] the final hydrogen shift to yield a loosely bound molecule of carbonic acid requires almost no activation energy.

The product complexes **11a** and **11b** are very similar both in structure and energy and only differ in the orientation of one OH group in the carbonic acid. Although a less stable isomer of carbonic acid is present in **11b**, we do not expect this to be problematic since isomerization should occur easily.

The energetically favored mechanism for formation of carbonic acid involves stabilization of **4** through bond rotation to yield **6**, followed by subsequent addition of a water molecule (**9b**) and a final proton transfer resulting in **11b**. An alternative mechanism in which the water molecule is added first (**4b**), followed by stabilization through bond rotation leading directly to **9b** is possible within the error margin of the applied B3LYP/6–311+G(d,p) level of theory. Regardless of the route to **9b**, product complex **11b** is always the result of the pathway.

Uncatalyzed reaction of COS with H_2O: Carbonyl sulfide in the gas phase reacts with water to yield carbon dioxide and hydrogen sulfide [Eq. (1)].

$$COS + H_2O \rightarrow CO_2 + H_2S \quad (1)$$

The reverse reaction, namely the nucleophilic attack of carbon dioxide by hydrogen sulfide, has been studied before.[27] We repeated these calculations at a higher level of theory [CCSD(T)/aug-cc-pV(Q+d)Z//B3LYP/aug-cc-pV(Q+d)Z] and performed a more extensive search of the energy hypersurface of this reaction (Scheme 3). We also report the results obtained at the B3LYP/6–311+G(d,p) level of theory to allow the reliability of this method to be assessed (Table 2). However, for the sake of clarity, all energies reported throughout this section are those obtained at the CCSD(T) level of theory, unless stated otherwise.

The unsymmetrical bonding pattern of COS means that nucleophilic attack by water can yield two different products depending on whether the C=O or the C=S bond is attacked. We did not succeed in locating an encounter complex (EC) for the initial approach of the reactants because of geometry convergence failure. Neither analytical recomputation of the gradients at each optimization step, nor variation of the descent routine employed altered this situation in the slightest. Our failure to find an EC is probably due to the bad description of long-range interactions achieved by most density functionals and thus must be regarded as an artifact of the applied method.

Table 2. Relative Gibbs' free energies and activation barriers for the gas-phase conversion of COS + H_2O into CO_2 + H_2S.

	ΔG [kcal mol^{-1}][a]	ΔG_a [kcal mol^{-1}][a]	ΔG [kcal mol^{-1}][b]	ΔG_a [kcal mol^{-1}][b]
H_2O + COS	0.0	–	0.0	–
12a (ts)	53.2	53.2	53.4	53.4
12a-w[c] (ts)	–	–	43.2	43.2
12b (ts)	63.3	63.3	63.7	63.7
12b-w[c] (ts)	–	–	47.4	47.4
13a	13.0	–	14.8	–
13b	22.7	–	24.9	–
14a (ts)	20.4	7.4	22.3	7.5
14c (ts)	22.6	9.6	24.8	10.0
15a	12.5	–	14.2	–
15c	18.0	–	20.3	–
16a (ts)	21.7	9.2	23.5	8.7
16c (ts)	21.4	3.4	23.5	3.2
17	16.1	–	18.2	–
18 (ts)	49.1	33.0	46.7	28.5
18-w[c] (ts)	–	–	37.5	19.3
CO_2 + H_2S	–7.7	–	–9.2	–

[a] Calculated at the CCSD(T)/aug-cc-pV(Q+d)Z//B3LYP/aug-cc-pV(Q+d)Z level of theory. [b] Calculated at the B3LYP/6–311+G(d,p)//B3LYP/6–311+G(d,p) level. [c] w, additional water molecule.

Nucleophilic attack by a water molecule on the C=S bond (path a) leads through the transition structure **12a** to intermediate **13a** and requires considerable activation energy (+53.2 kcal mol^{-1}, Table 2). This step is rate-determining for path a. Attack on the C=O bond (path b) requires additional energy to reach the transition structure **12b** and to form the product **13b** (+10 kcal mol^{-1} in each case compared to path a) and is clearly the less favorable pathway. Therefore, we did not investigate path b further. Addition to either of the two double bonds is simultaneous with a hydrogen transfer process and involves a four-membered cyclic transition structure in which the hydrogen atom is transferred while the π bond is broken.

We also investigated the effect of increasing the ring size in this ts from four to six by including a second molecule of water. We restricted all calculations involving an additional water molecule to the B3LYP/6–311+G(d,p) level of theory because of the increased size of the structures involved. In the presence of a second water molecule, the barrier for path a is decreased by 10 kcal mol^{-1} to 43.2 kcal mol^{-1}. The barrier for path b is reduced even more, but with an activation energy of 47.4 kcal mol^{-1} this process remains unfavorable. Correction of these values for estimated tunneling effects could result in even lower activation energies.[28] However, such calculations are very expensive and were beyond the scope of this study.

An additional reaction coordinate is opened up upon formation of **13a** since this complex can undergo rotation about either the C–S bond (continuation of path a) or the C–O bond (path c). Differentiation between paths a and c is

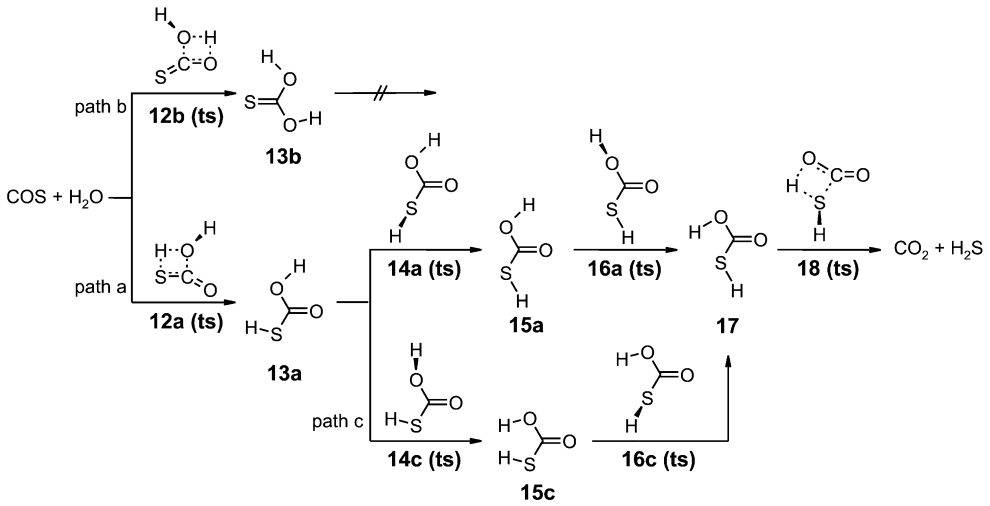

Scheme 3. The uncatalyzed gas-phase reaction of COS with H_2O.

not as easy as between a and b since path a is only slightly preferred over path c, both kinetically ($\delta\Delta G_a = 2.2$ kcal mol^{-1}; CCSD(T) level) and thermodynamically ($\delta\Delta G = 5.5$ kcal mol^{-1}; CCSD(T) level). In contrast to carbonic acid in the CO_2 pathway,[29] the *cis,cis*-isomer **15c** of the sulfur analogue is at an energy minimum on the potential energy surface.

Both isomers **15a** and **15c** have to undergo a second bond rotation about either the C–O or the C–S bond. This step is necessary since neither **15a** nor **15c** is aligned properly for direct decomposition to CO_2 and H_2S. Neither rotational pathway provides any substantial energetic hindrance to the formation of **17**, therefore both should be feasible. However, path a is somewhat more likely than path c since formation of **15a** is kinetically and thermodynamically slightly more favorable than formation of **15c**, as mentioned above.

A proton shift from the oxygen atom in **17** to the sulfur atom through a cyclic transition structure **18** yields the final reaction products CO_2 and H_2S. This transfer is simultaneous with the breaking of the C–S bond and the whole process is very similar to the addition of water to COS (first reaction step). Again, a substantial reaction barrier has to be overcome (33.0 kcal mol^{-1}) but this activation energy is still less than that required for the initial nucleophilic attack. As in the first step, this barrier is significantly reduced by the presence of a supporting second molecule of water, which effectively increases the ring size in the ts from four to six members. The activation energy for the water-assisted reaction with ts **18w** is 19.3 kcal mol^{-1} (calculated at the B3LYP/6–311+G(d,p) level of theory). As discussed above for the first step, the barrier for this last step would be lowered by tunneling effects.

We next searched for an encounter complex on the product side of the reaction. This time we succeeded in finding such a complex by using a smaller basis set for the conformational search. However, the energy of the complex showed a very strong basis-set dependency. A change of basis set from the very small split valence lanl2dz basis[30] (which contains neither polarization nor diffuse functions) to the medium-sized 6–311+G(d,p) and then the very large aug-cc-pV(Q+d)Z basis set caused an increase in the energy of the EC relative to the products from −0.8 to −0.3 to −0.1 kcal mol^{-1}. We therefore concluded that the encounter complex is an artifact caused by basis set superposition error and omitted the EC in our calculated mechanism.

We do not doubt the existence of encouter complexes on both the educt and the product side of the reaction. However, we were not able to identify any such complexes reliably at the B3LYP level of theory. In contrast, we had no problem locating an encounter complex for the nucleophilic attack with ts **12a** at the MP2/6-311+G(d,p) level of theory. Since the main focus of the work reported herein is the zinc-catalyzed reactions, and given the significant computional cost of recomputing all stationary points, we do not feel that ommitting the ECs for this uncatalyzed reaction causes serious problems.

Like the formation of carbonic acid, formation of thiol carbonic acid is endothermic. However, the reaction of COS resulting in CO_2 and H_2S is exothermic overall (−7.7 kcal mol^{-1}), while the corresponding reaction of CO_2 is thermodynamically neutral as a result of the identity of the educts and products.

All the results described above were well reproduced by the B3LYP/6–311+G(d,p) level of theory. The root-mean-square error (RMSE) of these results compared to those obtained at the CCSD(T)/aug-cc-pV(Q+d)Z//B3LYP/aug-cc-pV(Q+d)Z level is 1.87 kcal mol^{-1} and the mean-signed error (MSE) is 1.14 kcal mol^{-1}. The error introduced by omitting the much more expensive CCSD(T) calculations is therefore on the order of 2 kcal mol^{-1} for this uncatalyzed reaction. However, we expect a greater deviation for zinc-containing systems.

Reaction of COS with $[(H_3N)_3ZnOH]^+$: We considered the reaction of COS with **1**, a system used to model carbonic anhydrase that has already been successfully applied in various theoretical studies.[12,21–23] The presence of the zinc ion limited our investigations to the B3LYP/6–311+G(d,p) level of theory. The computed reaction pathway is shown in Scheme 4, and structures and data relating to the reaction coordinate are given in Figure 2, Figure 3, and Table 3.

Table 3. Relative Gibbs' free energies and activation barriers for the $[(H_3N)_3ZnOH]^+$-mediated conversion of COS into CO_2, with production of $[(H_3N)_3ZnSH]^+$. Calculated at the B3LYP/6–311+G(d,p) level of theory.

	ΔG [kcal mol^{-1}]	ΔG_a [kcal mol^{-1}]
1 + COS	0.0	–
19a	6.0	–
19b	4.7	–
20a (ts)	20.1	14.1
20b (ts)	22.9	18.2
21a	3.1	–
21b	15.0	–
$\mathbf{22_{rot}}$ (ts)[a]	7.7	4.6
$\mathbf{22_{sh}}$ (ts)[b]	33.0	29.9
$\mathbf{22_{sh}}$**-w** (ts)[b]	11.3	8.2
23	−2.4	–
24 (ts)	7.4	9.8
25	−1.0	–
26 (ts)	36.0	37.0
26-w (ts)	19.8	20.8
27 + CO_2	−20.7	–

[a] rot refers to the ts of a bond rotation. [b] sh refers to the ts of a hydrogen shift.

The reaction begins when COS approaches the zinc complex. The asymmetry of COS means that there are two pathways for nucleophilic attack of COS by **1**. Path a corresponds to attack on the C=S and path b on the C=O bond. In contrast to our failure to identify ECs for the uncatalyzed reaction, we found two stable encounter complexes **19a** and **19b** for the initial approach of COS in this catalyzed reaction. These ECs differ only in the orientation of the heterocumulene with respect to the zinc complex. The formation of the ECs is somewhat endothermic (Table 3). **19b** is slightly more stable (1.3 kcal mol^{-1}) than **19a** as a result of the formation of hydrogen bridges between two of the ammonia molecules and the oxygen atom of COS in **19b**. The sulfur atom in **19a** does not form such bonds. The native enzyme

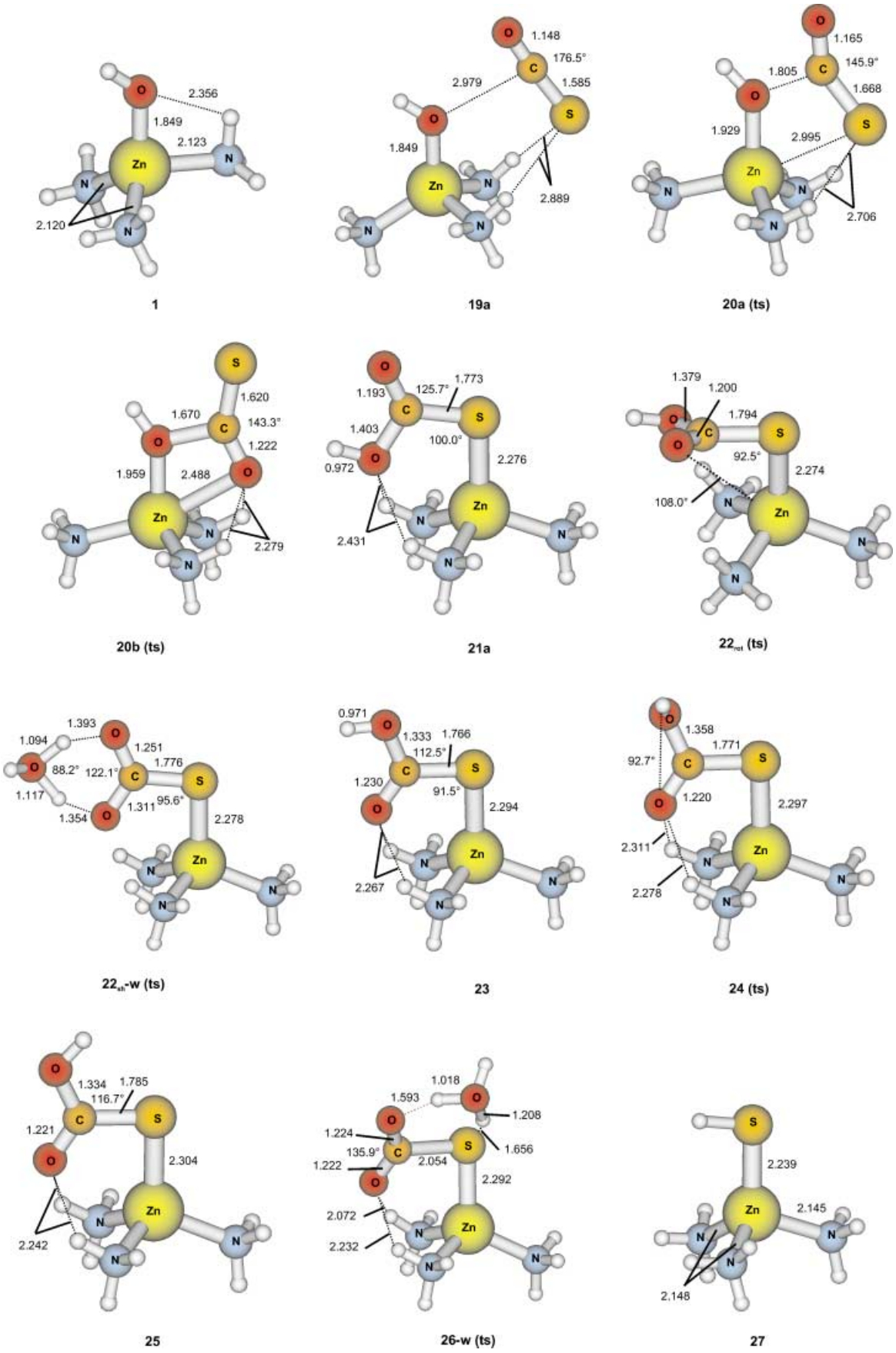

Figure 2. Structures of selected stationary points along the reaction coordinate of the reaction of $[(H_3N)_3ZnOH]^+$ (**1**) with COS (Scheme 4). Bond lengths are given in Å. Structures were calculated at the B3LYP/6–311+G(d,p) level of theory.

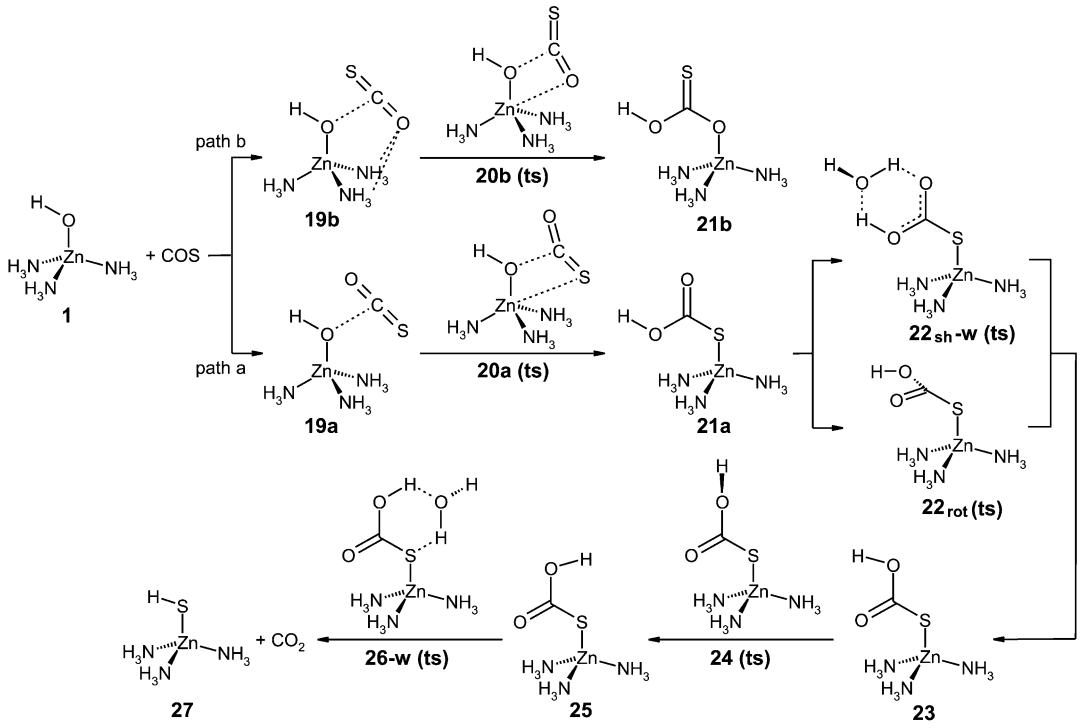

Scheme 4. Catalytic reaction of $[(H_3N)_3\,ZnOH]^+$ (**1**, a model of carbonic anhydrase) with COS.

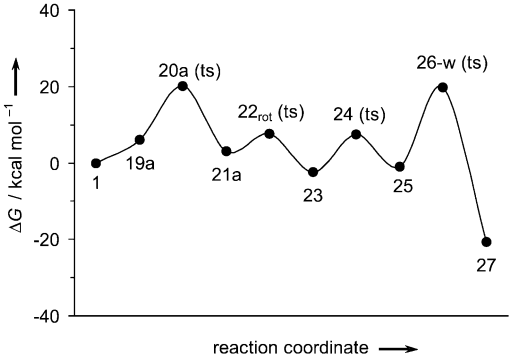

Figure 3. Gibbs' free energy as a function of the reaction coordinate of the most favorable path for the $[(H_3N)_3ZnOH]^+$-catalyzed conversion of COS and H_2O into CO_2 and H_2S. Calculated at the B3LYP/6–311+G(d,p) level of theory.

contains histidine residues, which cannot build such hydrogen bonds. We do not feel that the hydrogen bonds in **19b** are a significant problem since similar bridges were present in previous studies[18,21] on CO_2 fixation by **1** and the bonds did not alter the qualitative predictions made compared to those of a study with imidazole ligands instead of NH_3.[21] The error introduced by using NH_3 instead of imidazole was found to be 0.5–1.3 kcal mol^{-1},[21] which is comparable to the intrinsic error of the applied B3LYP/6–311+G(d,p) method.

The next step along the reaction coordinate is the nucleophilic attack of the carbon atom by the zinc-bound hydroxy group to form the Lindskog-type products **21a** and **21b**. Regardless of which double bond is attacked, the transition structure for nucleophilic addition (**20a** or **20b**) corresponds to a process in which the Zn–O bond and the π bond are broken with simultaneous formation of a Zn–X and a C–O bond. Attack on the C=S bond is kinetically ($\delta\Delta G_a = 2.8$ kcal mol^{-1}) and thermodynamically ($\delta\Delta G = 11.9$ kcal mol^{-1}) preferable to C=O bond attack. The same preference was found above for the uncatalyzed reaction. Possible reasons for destabilization of **21b** compared to **21a** are the lower affinity of zinc for oxygen than for sulfur, the bad overlap between the large sulfur and smaller carbon p orbitals forming the π bond, and better stabilization of **21a** by hyperconjugative effects. We did not follow path b any further since it is clearly less favorable than path a.

Nucleophilic attack by the zinc species on CO_2 has an activation energy of 15.0 kcal mol^{-1} in the gas phase and is thus the rate-determining step for CA.[18] The corresponding activation energy in the case of COS (path a) is 20.1 kcal mol^{-1}. The latter activation energy is clearly higher than that with CO_2 and we have not yet found kinetic proof of a preference of the catalyst for COS in the gas phase. However, as we demonstrate below, there is a strong thermodynamic preference for COS.

There are two mechanisms (Lindskog, a bond rotation around the C–S bond, and Lipscomb, a hydrogen shift from one oxygen atom to the other) by which **21a** can be converted into **23**. The transition structures for the rotation ($\mathbf{22_{rot}}$) and the hydrogen shift ($\mathbf{22_{sh}}$) are very similar to those found in the carbonic anhydrase cycle[18] except that the zinc-bound oxygen atom has been replaced by sulfur. In analogy to the CA reaction, the bond rotation mechanism ($\Delta G_a = 4.6$ kcal mol^{-1}) is strongly preferred over a hydrogen shift ($\Delta G_a = 29.9$ kcal mol^{-1}) when no supporting water molecule is present. The Lipscomb product **23** lies 2.4 kcal mol^{-1}

lower in energy than the separate reactants (see Figure 3). This result is in direct contrast to the situation in CO_2 fixation, where the Lipscomb product **6** is 3.1 kcal mol^{-1} higher in energy than the reactants.

The activation barrier for the Lipscomb mechanism is reduced by almost 20 kcal mol^{-1} to 8.2 kcal mol^{-1} if a water molecule mediates the proton shift. Again, estimation of tunneling corrections was beyond the scope of the present study. However, the imaginary frequency of **22$_{sh}$-w** (1052*i* cm^{-1}) indicates a rather narrow reaction profile and hence tunneling effects should not be negligible. The activation barrier for the proton shift could therefore be comparable to that for bond rotation. At this point, we cannot decide which of the two mechanisms is the preferred one. However, if tunneling effects are disregarded, rotation about the C–O bond (**22$_{rot}$**) is clearly preferred. Since the Lipscomb and Lindskog mechanisms lead to the same product, the outcome of this question does not affect the remaining part of the reaction and **23** is always formed.

To induce loss of CO_2, it is necessary to bring the OH group into the neighborhood of the sulfur atom (conformer **25**), which is easily accomplished by another bond rotation through transition structure **24**. The last step along the reaction coordinate involves a proton transfer from an oxygen to a sulfur atom, coupled with a bond rotation about the C–S bond to yield the zinc–sulfur complex **27** and CO_2.

The proton shift involves a four-membered ring intermediate and has a substantial activation energy of 36.0 kcal mol^{-1}, which is clearly much too high for an enzymatic process. Inclusion of an additional water molecule from the surrounding medium in the ts leads to **26-w**. The energy barrier is thus reduced to 19.8 kcal mol^{-1} and is expected to be lowered further by tunneling effects.

Figure 3 reveals that, as in the CA cycle, the nucleophilic attack of COS is rate determining for the COS reaction. As mentioned above, the activation barrier calculated for this step ($\Delta G_a = 20.1$ kcal mol^{-1}) is relatively high for an enzymatic process but is comparable with the gas-phase results for the CA cycle (15.0 kcal mol^{-1}). We assume that solvent effects significantly decrease this barrier, as in the fixation of CO_2.[18]

As calculated for the uncatalyzed reaction, the catalyzed reaction is exothermic overall and the final products are 20.7 kcal mol^{-1} more stable than the separate reactants. The thermodynamic stability of the products controls this process. The calculated exothermicity of the reaction is in complete agreement with the results of experimental COS fixation by CA-biomimetic systems. Simple zinc–pyrazolylborate complexes react quantitatively with COS to yield complexes containing a ZnSH moiety, as in **27**.[22]

What are the properties of the zinc sulfur complex **27**? Is this complex able to initiate its own catalytic cycle? The answers to these questions are discussed below.

Reaction of CO_2 with $[(H_3N)_3ZnSH]^+$: We considered the effect on the catalytic cycle when the source of sulfur is the catalyst instead of the cumulene. Replacement of the oxygen atom in **1** with sulfur and reoptimization of the structure leads to the catalyst $[(H_3N)_3ZnSH]^+$ (**27**; Scheme 5), for which we calculated the mechanism of CO_2 fixation in the gas phase at the B3LYP/6–311+G(d,p) theory level. This reaction can be interpreted both as an (theoretical) independent catalytic cycle and as a regeneration mechanism for the active catalyst in the reaction of **1** with COS.

In analogy to all the related CA model systems studied so far, an encounter complex **28** is formed in the first step of the reaction (Scheme 5, Figure 4). EC **28** lies 4.7 kcal mol^{-1} above the energy level of the separate reactants (Table 4). Nucleophilic attack of the carbon atom in CO_2 by the sulfur atom of **27** leads to a pentacoordinated trigonal bipyramidal transition structure **29** (+33.6 kcal mol^{-1}). This process is analogous to the nucleophilic attack of CO_2, CS_2, or COS by **1**; C–S and Zn–O bond formation is simultaneous with Zn–S and C=O bond breakage. The energy required for this step is approximately twice that necessary for nucleophilic attack of CO_2 by **1**. This result demonstrates how efficiently nature tuned the $[L_3ZnOH]^+/CO_2/H_2O$ system during the evolutionary process.

Table 4. Relative Gibbs' free energies and activation barriers for the $[(H_3N)_3ZnSH]^+$-mediated conversion of CO_2 into thiocarbonic acid. Calculated at the B3LYP/6–311+G(d,p) level of theory.

	ΔG [kcal mol^{-1}]	ΔG_a [kcal mol^{-1}]
27 + CO_2	0.0	-
28	4.7	–
29 (ts)	33.6	28.9
30a	30.2	–
30b (ts)	39.1	–
31 (ts)	58.0	27.8
32	25.3	–
33 (ts)	32.1	1.9
34	20.8	–
35 (ts)	55.0	34.2
36	35.8	–
37 (ts)	30.3	9.5
38	21.0	–
39a	23.3	–
39b	23.1	–
39c	21.0	–
40a (ts)	33.9	10.6
40b (ts)	35.3	12.2
40c (ts)	21.7	0.7
41a	19.8	–
41b	20.9	–
41c	22.1	–
27 + **13a**	24.1	–
27 + **15a**	23.4	–
1 + **13a**	35.8	–
1 + CO_2 + H_2S	11.2	–

We tried to identify an alternative mechanism in which the reaction starts with direct coordination of a water molecule to the central zinc atom in **27**. However, we were not able to find such a pentacoordinated structure. This difficulty may be due to the nature of the chosen ligand (NH_3), since we have not been able to locate a structure in which four ammonia molecules coordinate a ZnSH moiety either. We therefore conclude that, within the limitations of the applied model, such a mechanism is rather unlikely.

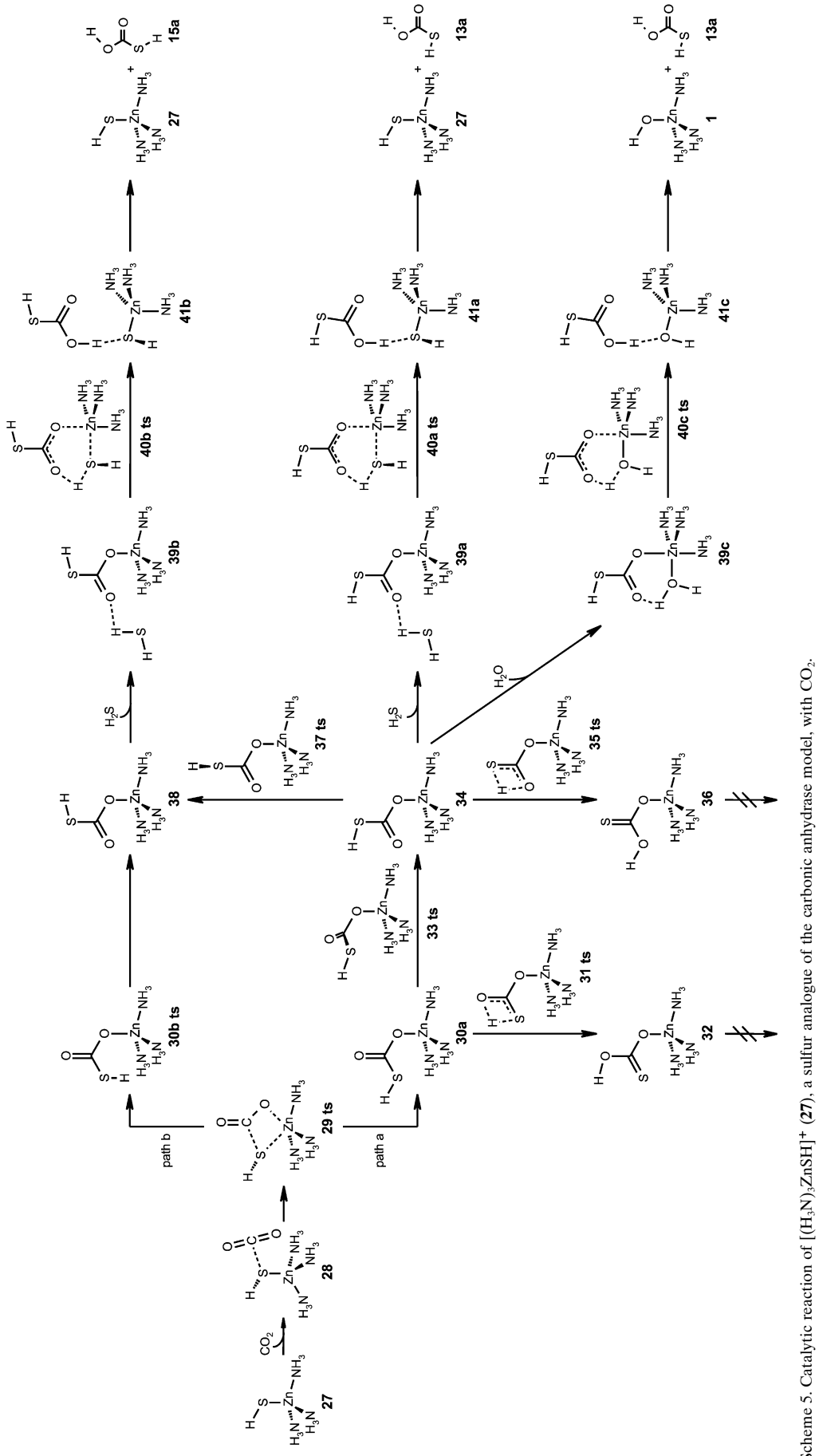

Scheme 5. Catalytic reaction of $[(H_3N)_3ZnSH]^+$ (**27**), a sulfur analogue of the carbonic anhydrase model, with CO_2.

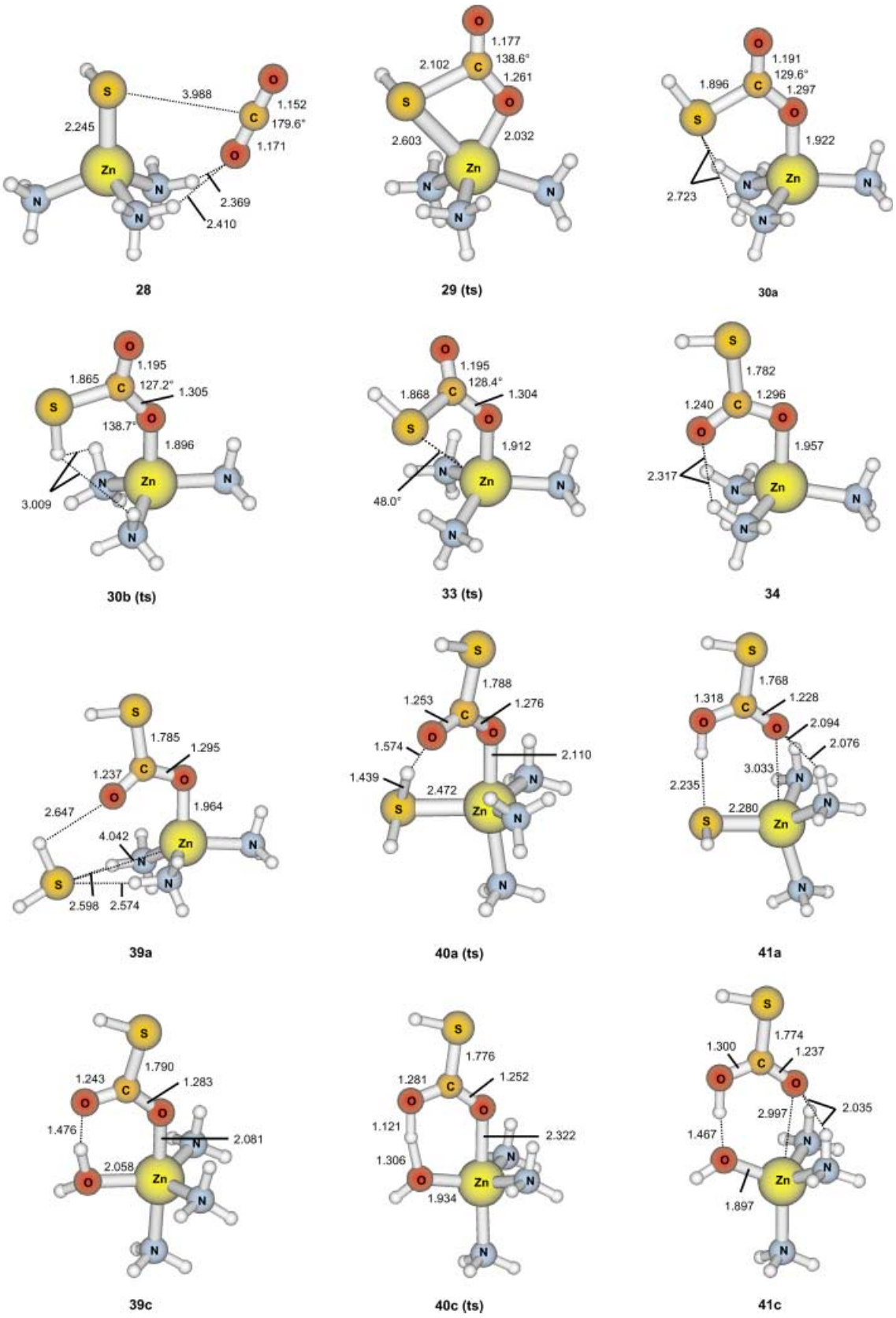

Figure 4. Structures at selected stationary points along the reaction coordinate of the reaction between $[(H_3N)_3ZnSH]^+$ (**27**) and CO_2 (Scheme 5). Bond lengths are given in Å. Structures were calculated at the B3LYP/6–311+G(d,p) level of theory.

Structure **29** undergoes an inversion process at the sulfur atom and can thus decompose into two different products, **30a** and **30b** (resolution of this coupled state was not possible at the B3LYP/6–311+G(d,p) level of theory). Species **30b** is not at an energetic minimum because of steric hindrance, but is instead a transition state for rotation about the C–O(Zn) bond. The pathway through **30b** leads to **38**. The transition structure **30b** lies 39.1 kcal mol^{-1} above the energy level of the separate reactants and we do not believe that this is an important pathway on the hypersurface of the gas-phase reaction.

The alternative species, **30a**, is at an energetic minimum and corresponds to a Lindskog-type intermediate in which an oxygen atom has replaced the original sulfur atom in the ligand sphere of zinc. As would be expected from the affinity of zinc for sulfur, **30a** has a considerably higher free energy than **28** (only 3.4 kcal mol^{-1} lower than the energy of the transition structure **29**). The influence of the sulfur atom in **30a** on the Zn–O bond is very small; the Zn–O bond distances in **30a** and **4** (CA; Scheme 1) differ by only 0.004 Å. The Zn–O bond is mainly electrostatic in nature, as indicated by the high negative charge (−0.96 e) on the oxygen atom.

Intermediate **30a** can undergo reaction by the Lipscomb (hydrogen shift) or the Lindskog (rotation) mechanism. This complex is the first structure reported herein from which these two pathways produce different products (**32** and **34**). This effect is the result of the unsymmetrical bonding pattern of the carbon atom (Scheme 5). In analogy to the results described above for similar systems, bond rotation (Lindskog mechanism) was found to be both kinetically and thermodynamically preferred and requires an activation energy of only 1.9 kcal mol^{-1} to generate the rotational isomer **34**. A proton shift (Lipscomb mechanism) to generate **32** is considerably less attractive and requires 27.8 kcal mol^{-1} for activation ($\delta\Delta G_a = 25.9$ kcal mol^{-1}). We avoided the inclusion of an external H_2X molecule in our calculations (see the preceding sections) and did not estimate tunneling effects. However, we expect tunneling to play an important role. Upon lowering of the energy of **31** through tunneling, an additional reaction channel may open up. This possibility would be an interesting topic for experimental investigation.

The rotational isomer **34** can again undergo either a bond rotation (leading to intermediate **38**) or a hydrogen shift (yielding compound **36**). As in the previous step in the mechanism, the rotation is clearly preferred over the hydrogen shift ($\delta\Delta G_a = 24.7$ kcal mol^{-1} for the two processes). In addition, **36** lies considerably higher in energy than **38**. As for the first proton shift, the inclusion of tunneling effects in calculations would lower the barrier significantly, which may make the reaction path leading to **38** competitive. However, we did not pursue the reaction channels leading to **32** and **36** any further because of the endothermic nature of these processes.

Isomers **34** and **38** differ only in the position of the S–H bond (*cis* or *trans*) with respect to the C–O(Zn) bond axis and are almost isoenergetic. Both isomers may be expected to be involved in the catalytic mechanism. In analogy to CO_2 fixation on **1**, CO_2 fixation on **27** requires an external heteroatom source to complete the hypothetical catalytic cycle and regenerate the catalyst. For carbonic anhydrase, this heteroatom source is clearly water (oxygen source). We investigated both H_2S and H_2O as external sources for **27**.

As an H_2S molecule approaches either **34** or **38**, an encounter complex (**39a** or **39b**) is formed in which a Lewis acid–base interaction occurs. The polarizability of H_2S appears to be sufficient to make this interaction possible. Water is not polarizable enough so no such EC could be found in the carbonic anhydrase cycle; instead, the pentacoordinated species **9b** (Scheme 2) is formed in which a strong Zn–OH_2 coordination is present. Such pentacoordinated complexes (**40a/b**) do not lie at minima on the hypersurface of the thio analogue but are cyclic transition structures, each with a six-membered ring. These complexes are the transition structures of a synchronous Zn–S bond formation/Zn–O cleavage process accompanied by hydrogen transfer to the loosely bound thiocarbonic acid. The encounter complex thus goes through **40a/b** straight to a product complex **41a/b** instead of passing through an additional stable intermediate. This step requires 10.6 kcal mol^{-1} for activation.

As expected for steric reasons, we were not able to locate a transition structure in which both H_2S and HSC(O)O are in an equatorial position. Complexes with both H_2S and HSC(O)O in an axial position lack the ability to undergo a proton transfer and we did not consider such structures. However, such complexes cannot be fully excluded since it is known that internal rotations can occur in pentacoordinated zinc complexes.

In the product complexes **41a/b**, the thiocarbonic acid is only loosely bound to the regenerated active catalyst **27** through a hydrogen bond. The final dissociation of thiocarbonic acid requires only 4.3 kcal mol^{-1} (path a) or 2.5 kcal mol^{-1} (path b), much lower energies than required by the corresponding step in the carbonic anhydrase cycle (26.2 kcal mol^{-1} in the gas phase).[18] Clearly, an assisting external base is not needed in this case. The overall reaction ($\Delta G = +24.1$ kcal mol^{-1}) resulting in **27** and **13a/15a** is endothermic because the free energy of thiocarbonic acid is greater than the sum of the energies of the separate reactants CO_2 and H_2S.

In conclusion, the overall activation barrier of the catalytic cycle is 33.9 kcal mol^{-1}, which is rather high for an enzymatic process. However, it should be possible to access this reaction experimentally, especially the stoichiometric reaction in which no regeneration of the catalyst is necessary. We are now investigating whether or not we can overcome this barrier experimentally by modifying our biomimetic zinc complexes and varying the temperature and/or pressure. In a similar study, pyrazolylborate-type model systems showed no reactivity towards heterocumulenes at ambient pressure and temperature.[31]

When H_2O was used as the heteroatom source instead of H_2S, a new reaction channel opened up that results in **1** and thiocarbonic acid (Scheme 5 and Figure 5). Interaction of **34** and H_2O leads to pentacoordinated **39c** in which the water molecule directly coordinates the central zinc atom. Com-

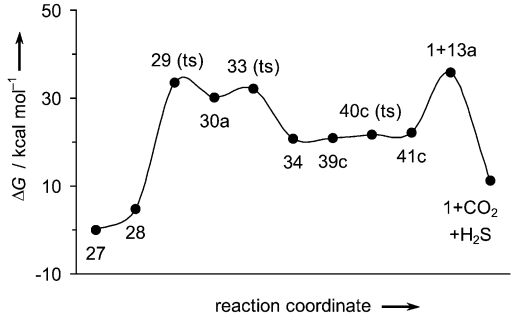

Figure 5. Gibbs' free energy as a function of the reaction coordinate for the most favorable path for the conversion of $[(H_3N)_3ZnSH]^+$ into $[(H_3N)_3ZnOH]^+$ by CO_2 and H_2O. Calculated at the B3LYP/6–311+G(d,p) level of theory.

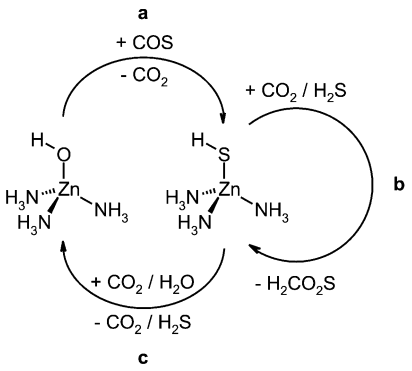

Scheme 6. Schematic depiction of the reaction paths reported herein.

plex **39c** is only 0.2 kcal mol^{-1} higher in energy than **34** and thus formation of **39c** is preferred over formation of **39a**. A proton shift with ts **40c** yields the product complex **41c** and requires almost no activation. Therefore, **39c** and **41c** should be in equilibrium. The calculated energy difference between these complexes is much smaller than the accuracy of the applied B3LYP method so we can neither state definitely which of **39c** and **41c** is more stable nor give an accurate value for the reaction barrier. Coupled cluster [CCSD(T)] single points would give more reliable results but such calculations were not possible with our computational resources. Dissociation into the free catalyst **1** and thiocarbonic acid **13a** requires 13.7 kcal mol^{-1}. This activation energy does not seem to be a problem since mechanisms similar to those previously reported[18] should decrease its value. Complex **1** can restart the reaction cascade described in Scheme 4, that is, the transformation of COS. The thiocarbonic acid **13a** readily decomposes into CO_2 and H_2S. Thus, the CO_2 molecule mediates the conversion of $[(H_3N)_3ZnSH]^+$ (**27**) and H_2O into $[(H_3N)_3ZnOH]^+$ (**1**) and H_2S. This reaction is slightly endothermic overall (+11.2 kcal mol^{-1}).

Conclusion

Why does nature prefer the $[L_3Zn{-}OH]^+/CO_2/H_2O$ system to all the other conceivable $[L_nZn{-}XH]^+/X{=}C{=}Y/H_2X$ (X = O, S) combinations? From the results of the investigation described herein (summarized in Scheme 6), we conclude that a variety of structural and energetic properties are optimized in the natural system.

The calculated reaction path for COS (a in Scheme 6) leads to the $[(H_3N)_3ZnSH]^+$ complex and CO_2. Nucleophilic attack is the rate-determining step of the catalytic cycle for both CO_2 and COS. However, there are differences in the mechanistic details of the cycles of these two compounds. The hydration of CO_2 is an endergonic process, while the catalytic hydration of COS is exergonic.

Surprisingly, the zinc-bound sulfur atom in $[(H_3N)_3ZnSH]^+$ is capable of attacking CO_2 (b in Scheme 6), although the activation barrier is rather high for a biological process under standard ambient conditions. However, under more extreme conditions such a catalytic cycle is a realistic possibility. Replacement of H_2S with water indicates that, if nucleophilic attack on CO_2 takes place, it is generally possible to regenerate the $[L_3ZnOH]^+$ catalyst found in the native enzyme (c in Scheme 6).

Nature has chosen an elegant and efficient system, the $[L_3ZnOH]^+/CO_2/H_2O$ group of reactants. Although this system has a certain sensitivity to COS, the catalyst can be regenerated at a characteristic stage of the cycle. As a result of the higher energies involved with COS than with CO_2, the regeneration is likely to be relatively slow in the presence of COS. However, this pathway would prevent the disastrous permanent deactivation of carbonic anhydrase upon reaction with COS. This finding is of special interest as COS is consumed by the biosphere (i.e. terrestrial vegetation, leaf litter, soil, alga, lichens), where irreversible inhibition of CA would immediately reduce or even prevent the vital exchange of CO_2.

Some of the results presented herein should be transferable to stoichiometric syntheses that follow the reaction pathways of carbonic anhydrase. The reactivity of zinc-bound hydrogen sulfide and its variants as sulfur analogues of carbonic anhydrase is the subject of ongoing research activities.

Computational Methods

Full geometry optimizations (i.e. without symmetry constraints) were carried out with the GAUSSIAN98 program package.[32] Depending on the size of the system being studied, various calculation methods and basis sets were employed. All geometry optimizations reported herein were performed by using the hybrid B3LYP[33] density functional method, which includes the use of a term that accounts for the effects of dynamic electron correlation (Coulomb hole).[34] Reaction hypersurfaces that did not contain zinc were optimized at the B3LYP/aug-cc-pV(Q+d)Z level of theory and those containing zinc at the somewhat lower-standard B3LYP/6–311+G(d,p) level. The aug-cc-pV(Q+d)Z basis set employed differs from the standard aug-cc-pVQZ basis set of Dunning et al.[35] in that it includes an additional high-exponent *d* function for second-row atoms to account for core polarization effects.[36] The B3LYP/aug-cc-pV(Q+d)Z level of theory generally yields quite accurate results.[37] Even more accurate energies were calculated for small systems (mostly relevant for the uncatalyzed reactions or for reference energies) by using the coupled cluster CCSD(T)/aug-cc-pV(Q+d)Z single point method[38] and a B3LYP/aug-cc-pV(Q+d)Z optimal geometry. The energies calculated at the B3LYP/aug-cc-pV(Q+d)Z level differ at most by approximately 3 kcal mol^{-1} from the results of the much more expensive coupled

cluster method. The error introduced by omitting the very expensive CCSD(T) calculations is therefore less than 3 kcal mol^{-1}. Although a correlation-consistent basis set of triple zeta valence quality (cc-pVTZ) with an effective core potential has recently been published for zinc,[39] our own investigations[40] show that the use of this basis set for the systems under consideration does not lead to substantial improvements in the results compared to those obtained from the B3LYP/6–311+G(d,p) level of theory. We therefore restricted our investigations on hypersurfaces containing zinc to the B3LYP/6–311+G(d,p) level of theory. All calculated stationary points were rigorously characterized as minima or transition structures according to the number of imaginary modes by applying a second-order derivative calculation (vibrational analysis) at the same level of theory as that at which the optimization was performed. Visualization of the reactive modes of the transition structures (with VIEWMOL[41] and MOLDEN[42] software) was used to support the assignment of energetic minimum structures versus transition structures. All energies reported are Gibbs' free enthalpies with zero-point energy corrections, as well as thermal (ΔH) and entropic ($T\Delta S$) corrections calculated by the standard thermodynamic routines in GAUSSIAN98 for standard ambient temperature and pressure conditions. The natural bond orbital analysis of Reed and Weinhold[43] was applied to calculate bond orders, atomic charges, and orbital energies for selected intermediates.

Acknowledgments

Financial support by the Deutsche Forschungsgemeinschaft (Collaborative Research Centre 436, University of Jena, Germany), the Fonds der Chemischen Industrie (Germany), and the Thüringer Ministerium für Wissenschaft, Forschung und Kunst (Erfurt, Germany) is gratefully acknowledged. We thank Dr. J. Weston (Jena, Germany) for helpful and stimulating discussions and for help with preparing the manuscript. We would also like to thank Hewlett-Packard for support.

[1] a) R. P. Davis, *J. Am. Chem. Soc.* **1958**, *80*, 5209–5214; b) J. E. Coleman in *Zinc Enzymes* (Eds.: I. Bertini, C. Luchinat, W. Maret, M. Zeppezauer), Birkhauser, Boston, **1986**, pp. 49–58; c) S. Lindskog in *Zinc Enzymes* (Eds.: I. Bertini, C. Luchinat, W. Maret, M. Zeppezauer), Birkhauser, Boston, **1986**, pp. 307–316; d) H. Steiner, B. H. Jonsson, S. Lindskog, *FEBS Lett.* **1976**, *62*, 16–20; e) D. N. Silverman, S. Lindskog, C. K. Tu, G. C. Wynns, *J. Am. Chem. Soc.* **1979**, *101*, 6734–6740; f) R. S. Rowlett, D. N. Silverman, *J. Am. Chem. Soc.* **1982**, *104*, 6737–6741; g) I. Bertini, C. Luchinat, *Acc. Chem. Res.* **1983**, *16*, 272–279; h) S. Lindskog in *Carbonic Anhydrase* (Ed. S. Lindskog), Wiley, New York, **1983**, p. 77; i) D. N. Silverman, S. Lindskog, *Acc. Chem. Res.* **1988**, *21*, 30–36; j) J. Y. Liang, W. N. Lipscomb, *Biochemistry* **1988**, *27*, 8676–8682; and references cited therein.

[2] A. J. Kettle, U. Kuhn, M. von Hobe, J. Kesselmeier, M. O. Andreae, *J. Geoph. Res. Atmos.* **2002**, *107*, 4658, DOI 10.1029/2002 JD002187.

[3] a) J. Kesselmeier, A. Hubert, *Atmos. Environ.* **2002**, *36*, 4679–4686; b) U. Kuhn, J. Kesselmeier, *J. Geophys. Res. Atmos.* **2000**, *105*, 26783–26792; c) S. Blezinger, C. Wilhelm, J. Kesselmeier, *Biogeochemistry* **2000**, *48*, 185–197; d) U. Kuhn, A. Wolf, C. Gries, T. H. Nash III, J. Kesselmeier, *Atmos. Environ.* **2000**, *34*, 4867–4878; e) U. Kuhn, C. Ammann, A. Wolf, F. X. Meixner, M. O. Andreae, J. Kesselmeier, *Atmos. Environ.* **1999**, *33*, 995–1008; f) J. Kesselmeier, N. Teusch, U. Kuhn, *J. Geoph. Res. Atmos.* **1999**, *104*, 11577–11584; g) G. Protoschill-Krebs, C. Wilhelm, J. Kesselmeier, *Atmos. Environ.* **1996**, *30*, 3151–3156; h) G. Protoschill-Krebs, C. Wilhelm, J. Kesselmeier, *Botanica Acta* **1995**, *108*, 445–448; i) G. Protoschill-Krebs, J. Kesselmeier, *Botanica Acta* **1992**, *105*, 206–212.

[4] P. Woolley, *Nature* **1975**, *258*, 677–682.

[5] J. Y. Liang, W. N. Lipscomb, *Int. J. Quant. Chem.* **1989**, 36, 299–312.

[6] a) A. Liljas, K. K. Kannan, P. C. Bergsten, I. Waara, K. Fridborg, B. Strandberg, U. Carlbom, L. Jarup, S. Lovgren, M. Petef, *Nature New Biol.* **1972**, *235*, 131–137; b) A. E. Eriksson, T. A. Jones, A. Liljas, *Proteins* **1988**, *4*, 274–282; c) K. Håkansson, M. Carlsson, L. A. Svensson, A. Liljas, *J. Mol. Biol.* **1992**, *227*, 1192–1204; d) Y. Xue, J. Vidgren, L. A. Svensson, A. Liljas, B. H. Jonsson, S. Lindskog, *Proteins* **1993**, *15*, 80–87; e) R. S. Alexander, L. L. Kiefer, C. A. Fierke, D. W. Christianson, *Biochemistry* **1993**, *32*, 1510–1518; f) J. A. Ippolito, D. W. Christianson, *Biochemistry* **1993**, *32*, 9901–9905; g) L. L. Kiefer, J. A. Ippolito, C. A. Fierke, D. W. Christianson, *J. Am. Chem. Soc.* **1993**, *115*, 12581–12582; h) L. L. Kiefer, J. F. Krebs, S. A. Paterno, C. A. Fierke, *Biochemistry* **1993**, *32*, 9896–9900; i) B. L. Vallee, D. S. Auld, *Acc. Chem. Res.* **1993**, *26*, 543–551; j) J. A. Ippolito, D. W. Christianson, *Biochemistry* **1994**, *33*, 15241–15249; k) C. A. Lesburg, D. W. Christianson, *J. Am. Chem. Soc.* **1995**, *117*, 6838–6844; l) L. R. Scolnick, A. M. Clements, J. Liao, L. Crenshaw, M. Hellberg, J. May, T. R. Dean, D. W. Christianson, *J. Am. Chem. Soc.* **1997**, *119*, 850–851; and references cited therein.

[7] a) D. W. Christianson, C. A. Fierke, *Acc. Chem. Res.* **1996**, *29*, 331–339; b) D. Duda, C. Tu, D. N. Silverman, A. J. Kalb (Gilboa), M. Agbandje-McKenna, R. McKenna, *Protein Pept. Lett.* **2001**, *8*, 63–67; c) D. Duda, C. Tu, M. Qian, P. Laipis, M. Agbandje-McKenna, D. N. Silverman, R. McKenna, *Biochemistry* **2001**, *40*, 1741–1748; d) H. An, C. Tu, D. Duda, I. Montanez-Clemente, K. Math, P. J. Laipis, R. McKenna, D. N. Silverman, *Biochemistry* **2002**, *41*, 3235–3242.

[8] S. Lindskog, L. Henderson, K. K. Kannan, A. Liljas, P. O. Nyman, B. Strandberg in *The Enzymes, Vol. 5* (Ed.: P. Boyer), 3rd ed., Academic Press, New York, **1971**, p. 587.

[9] a) S. Lindskog, A. Liljas, *Curr. Opin. Struct. Biol.* **1993**, *3*, 915–920; b) X. Zhang, C. D. Hubbard, R. van Eldik, *J. Phys. Chem.* **1996**, *100*, 9161–9171; c) H. C. Lee, Y. H. Ko, S. B. Baek, D. H. Kim, *Bioorg. Med. Chem. Lett.* **1998**, *8*, 3379–3384, and references cited therein.

[10] a) K. M. Merz, Jr., *J. Mol. Biol.* **1990**, *214*, 799–802; b) K. M. Merz, Jr., *J. Am. Chem. Soc.* **1991**, *113*, 406–411; c) K. M. Merz, Jr., L. Banci, *J. Phys. Chem.* **1996**, *100*, 17414–17420; d) K. M. Merz, Jr., L. Banci, *J. Am. Chem. Soc.* **1997**, *119*, 863–871; e) S. Toba, G. Colombo, K. M. Merz, Jr., *J. Am. Chem. Soc.* **1999**, *121*, 2290–2302.

[11] a) K. M. Merz, Jr., R. Hoffmann, M. J. S. Dewar, *J. Am. Chem. Soc.* **1989**, *111*, 5636–5649; b) A. Alex, T. Clark, *J. Comp. Chem.* **1992**, *13*, 704–717; c) S. Alvarez-Santos, A. González-Lafont, J. M. Lluch, B. Oliva, F. X. Avilés, *Can. J. Chem.* **1994**, *72*, 2077–2083; d) M. Sakurai, T. Furuki, Y. Inoue, *J. Phys. Chem.* **1995**, *99*, 17789–17794; e) M. Hartmann, K. M. Merz, Jr., R. van Eldik, T. Clark, *J. Mol. Model.* **1998**, *4*, 355–365.

[12] a) A. Pullman, D. Demoulin, *Int. J. Quant. Chem.* **1979**, *16*, 641–653; b) J. Y. Liang, W. N. Lipscomb, *J. Am. Chem. Soc.* **1986**, *108*, 5051–5058; c) J. Y. Liang, W. N Lipscomb, *Biochemistry* **1987**, *26*, 5293–5301; d) I. Bertini, C. Luchinat, M. Rosi, A. Sgamellotti, F. Tarantelli, *Inorg. Chem.* **1990**, *29*, 1460–1463; e) M. Krauss, D. R. Garmer, *J. Am. Chem. Soc.* **1991**, *113*, 6426–6435; f) Y. J. Zheng, K. M. Merz, Jr., *J. Am. Chem. Soc.* **1992**, *114*, 10498–10507; g) D. R. Garmer, *J. Phys. Chem. B* **1997**, *101*, 2945–2953; h) S. Álvarez-Santos, A. González-Lafont, J. M. Lluch, *Can. J. Chem.* **1998**, *76*, 1027–1032; i) D. Lu, G. A. Voth, *J. Am. Chem. Soc.* **1998**, *120*, 4006–4014; j) C. Muguruma, *J. Mol. Struct. (THEOCHEM)* **1999**, *461/462*, 439–452.

[13] M. Hartmann, T. Clark, R. van Eldik, *J. Mol. Model.* **1996**, *2*, 1–4.

[14] a) A. Looney, R. Han, K. McNeil, G. Parkin, *J. Am. Chem. Soc.* **1993**, *115*, 4690–4697; b) N. Kitajima, S. Hikichi, M. Tanaka, Y. Moro-oka, *J. Am. Chem. Soc.* **1993**, *115*, 5496–5508; c) M. Sakurai, T. Furuki, Y. Inoue, *J. Phys. Chem.* **1995**, *99*, 17789–17794; d) C. Bazzicalupi, A. Bencini, A. Bencini, A. Bianchi, F. Corana, V. Fusi, C. Giorgi, P. Paoli, P. Paoletti, B. Valtancoli, C. Zanchini, *Inorg. Chem.* **1996**, *35*, 5540–5548; e) K. Nakata, M. K. Uddin, K. Ogawa, K. Ichikawa, *Chem. Lett.* **1997**, 991–992; f) D. H. Kim, S. J. Chung, E. J. Kim, G. R. Tian, *Bioorg. Med. Chem. Lett.* **1998**, *8*, 859–864; g) K. Ogawa, K. Nakata, K. Ichikawa, *Chem. Lett.* **1998**, 797–798.

[15] a) R. Alsfasser, M. Ruf, S. Trofimenko, H. Vahrenkamp, *Chem. Ber.* **1993**, *126*, 703–710; b) R. Gregorzik, U. Hartmann, H. Vahrenkamp, *Chem. Ber.* **1994**, *127*, 2117–2122; c) U. Hartmann, R. Gregorzik, H. Vahrenkamp, *Chem. Ber.* **1994**, *127*, 2123–2127; d) C. Titze, J. Hermann, H. Vahrenkamp, *Chem. Ber.* **1995**, *128*, 1095–1103; e) P. Gockel, R. Vogler, H. Vahrenkamp, *Chem. Ber.* **1996**, *129*, 887–895; f) P. Gockel, H. Vahrenkamp, *Chem. Ber.* **1996**, *129*, 1243–1249; g) M. Ruf, H. Vahrenkamp, *Chem. Ber.* **1996**, *129*, 1025–1028; h) M. Ruf, R. Burth, K. Weis, H. Vahrenkamp, *Chem. Ber.* **1996**, *129*,

1251 – 1257; i) M. Ruf, F. A. Schell, R. Walz, H. Vahrenkamp, *Chem. Ber./Receuil* **1997**, *130*, 101 – 104.
[16] a) E. Kimura, T. Koike, K. Toriumi, *Inorg. Chem.* **1988**, 27, 3687 – 3688; b) E. Kimura, H. Kurosaki, T. Koike, K. Toriumi, *J. Incl. Phenom. Mol. Recog. Chem.* **1992**, *12*, 377 – 387; c) E. Kimura, I. Nakamura, T. Koike, M. Shionoya, Y. Kodama, T. Ikeda, M. Shiro, *J. Am. Chem. Soc.* **1994**, *116*, 4764 – 4771; d) E. Kimura, *Prog. Inorg. Chem.* **1994**, *41*, 443 – 491; e) E. Kimura, T. Koike, *Adv. Inorg. Chem.* **1997**, *44*, 229 – 261; f) E. Kimura, T. Koike, M. Shionoya, *Struct. Bonding* **1997**, *89*, 1 – 28; g) E. Kimura, *Acc. Chem. Res.* **2001**, *34*, 171 – 179.
[17] a) X. Zhang, R. van Eldik, T. Koike, E. Kimura, *Inorg. Chem.* **1993**, *32*, 5749 – 5755; b) X. Zhang, R. van Eldik, *Inorg. Chem.* **1995**, *34*, 5606 – 5614; c) A. Schrodt, A. Neubrand, R. van Eldik, *Inorg. Chem.* **1997**, *36*, 4579 – 4584; d) Z.-W. Mao, G. Liehr, R. van Eldik, *J. Chem. Soc. Dalton Trans.* **2001**, 1593 – 1600.
[18] M. Mauksch, M. Bräuer, J. Weston, E. Anders, *ChemBioChem* **2001**, *2*, 190 – 198.
[19] J. B. Foresman, T. A. Keith, K. B. Wiberg, J. Snoonian, M. J. Frisch, *J. Phys. Chem.* **1996**, *100*, 16098 – 16104.
[20] C. Tu, B. C. Tripp, J. G. Ferry, D. N. Silverman, *J. Am. Chem. Soc.* **2001**, *123*, 5861 – 5866.
[21] M. Bräuer, J. L. Pérez-Lustres, J. Weston, E. Anders, *Inorg. Chem.* **2002**, *41*, 1454 – 1463.
[22] a) M. Rombach, H. Brombacher, H. Vahrenkamp, *Eur. J. Inorg. Chem.* **2002**, 153 – 159; b) M. Bräuer, E. Anders, S. Sinnecker, W. Koch, M. Rombach, H. Brombacher, H. Vahrenkamp, *Chem. Commun.* **2000**, 647 – 648.
[23] S. Sinnecker, M. Bräuer, W. Koch, E. Anders, *Inorg. Chem.* **2001**, *40*, 1006 – 1013.
[24] C. P. Rinsland, A. Goldman, E. Mahieu, R. Zander, J. Notholt, N. B. Jones, D. W. T. Griffith, T. M. Stephen, *J. Geophys. Res. Atmos.* **2002**, *107*, 4657, DOI 10.1029/2002 JD002522.
[25] P. J. Crutzen, *Geophys. Res. Lett.* **1976**, *3*, 73 – 76.
[26] D. J. Hofmann, S. Solomon, *J. Geophys. Res.* **1989**, *94*, 5029 – 5041.
[27] P. Sánchez-Andrada, I. Alkorta, J. Elguero, *J. Mol. Struct. (THEOCHEM)* **2001**, *544*, 5 – 23.
[28] Q. Cui, M. Karplus, *J. Phys. Chem. B* **2003**, *107*, 1071 – 1078.
[29] M. Bräuer, **2000**, Ph.D. Thesis, Friedrich-Schiller-Universität, Jena (Germany).
[30] T. H. Dunning, Jr., P. J. Hay in *Modern Theoretical Chemistry, Vol. 3* (Ed.: H. F. Schaefer II), Plenum, New York, **1976** p. 1.
[31] M. Rombach, H. Vahrenkamp, *Inorg. Chem.* **2001**, *40*, 6144 – 6150.
[32] Gaussian 98, Revision A.11, M. J. Frisch, G. W. Trucks, H. B. Schlegel, G. E. Scuseria, M. A. Robb, J. R. Cheeseman, V. G. Zakrzewski, J. A. Montgomery Jr., R. E. Stratmann, J. C. Burant, S. Dapprich, J. M. Millam, A. D. Daniels, K. N. Kudin, M. C. Strain, O. Farkas, J. Tomasi, V. Barone, M. Cossi, R. Cammi, B. Mennucci, C. Pomelli, C. Adamo, S. Clifford, J. Ochterski, G. A. Petersson, P. Y. Ayala, Q. Cui, K. Morokuma, D. K. Malick, A. D. Rabuck, K. Raghavachari, J. B. Foresman, J. Cioslowski, J. V. Ortiz, A. G. Baboul, B. B. Stefanov, G. Liu, A. Liashenko, P. Piskorz, I. Komaromi, R. Gomperts, R. L. Martin, D. J. Fox, T. Keith, M. A. Al-Laham, C. Y. Peng, A. Nanayakkara, C. Gonzalez, M. Challacombe, P. M. W. Gill, B. Johnson, W. Chen, M. W. Wong, J. L. Andres, C. Gonzalez, M. Head-Gordon, E. S. Replogle, and J. A. Pople, Gaussian Inc., Pittsburgh PA, **1998**.
[33] A. D. Becke, *J. Chem. Phys.* **1993**, *98*, 5648 – 5652.
[34] C. Lee, W. Yang, R. G. Parr, *Phys. Rev. B.* **1988**, *37*, 785 – 789.
[35] R. A. Kendall, T. H. Dunning, Jr., R. J. Harrison, *J. Chem. Phys.* **1992**, *96*, 6796 – 6806.
[36] T. H. Dunning, Jr., K. A. Peterson, A. K. Wilson, *J. Chem. Phys.* **2001**, *114*, 9244 – 9253.
[37] K. S. Raymond, R. A. Wheeler, *J. Comp. Chem.* **1999**, *20*, 207 – 216.
[38] a) G. D. Purvis, R. J. Bartlett, *J. Chem. Phys.* **1982**, *76*, 1910 – 1918; b) G. E. Scuseria, C. L. Janssen, H. F. Schaefer III, *J. Chem. Phys.* **1988**, *89*, 7382 – 7387; c) G. E. Scuseria, H. F. Schaefer III, *J. Chem. Phys.* **1989**, *90*, 3700 – 3703; d) J. A. Pople, M. Head-Gordon, K. Raghavachari, *J. Chem. Phys.* **1987**, *87*, 5968 – 5975.
[39] J. M. L. Martin, A. Sundermann, *J. Chem. Phys.* **2001**, *114*, 3408 – 3420.
[40] S. Schenk, diploma thesis, **2001**, Friedrich-Schiller-Universität Jena (Germany).
[41] http://viewmol.sourceforge.net
[42] G. Schaftenaar, J. H. Noordik, *J. Comput.-Aided Mol. Design* **2000**, *14*, 123 – 134.
[43] a) A. E. Reed, L. A. Curtiss, F. Weinhold, *Chem. Rev.* **1988**, *88*, 899 – 926; b) A. E. Reed, L. R. B. Weinstock, F. Weinhold, *J. Chem. Phys.* **1985**, *83*, 735 – 746; c) A. E. Reed, F. Weinhold, *J. Chem. Phys.* **1983**, *78*, 4066 – 4073.

Received: November 3, 2003

Published online: May 6, 2004

